Bond-Energy and Surface-Energy Calculations in Metals

James G. Eberhart* and Steve Horner
Department of Chemistry, University of Colorado at Colorado Springs, Colorado Springs, Colorado 80933-7150
**jeberhar@uccs.edu*

One of the major goals of materials science is to relate the properties of materials to the potential functions that characterize the atomic and molecular interactions that hold the material together. Sharing this ambitious and ongoing quantum-mechanical program with students is usually beyond the scope of an introductory course in materials science. However, there are situations where an elementary approach to connecting atomic interactions to material properties is possible. One of these areas is the use of the lattice energies and bond energies of metals to predict the metal surface energies. These calculations are presented here at a level that is suitable for an introductory materials science course.

Many phenomena of importance in solids depend on the properties of the surfaces or interfaces of the materials in question, rather than properties of the bulk material. Surface and interfacial tensions are key properties in understanding phenomena such as crystal faceting, grain structure, crack propagation, capillarity-driven mass transport, vacancy formation, wetting, and adhesion *(1)*. The bonding concepts considered here are similar to those applied to the covalent bond energy that is a central idea in general, organic, inorganic, and physical chemistry courses *(2)*. Once determined, the metallic bond strengths are seen to be somewhat smaller than the energies of the more familiar covalent bonds. For body-centered cubic (bcc), face-centered cubic (fcc), and hexagonal-closest-packed (hcp) metals, the bond energy and the lattice constant can then be used to make reasonably good estimates the surface energies of solid metals.

Bond Energies for the Bcc and Fcc Metals

The calculation of the bond energy in a metallic lattice is similar to that in gaseous molecules except that students find it a little more challenging to determine the number of bonds broken during atomization. The atomization of a crystalline metal, M(c), can be represented by the process

$$\mathrm{M(c)} \rightarrow \mathrm{M(g)} \tag{1}$$

where the molar energy of atomization of the metal lattice is $\Delta_a U$ and the gaseous metal is assumed to be entirely monatomic. The atomization energy is also called the energy of sublimation, the cohesive energy, or the lattice energy. The calculation of bond energies from $\Delta_a U$ will initially be limited to bcc and fcc metals.

Each metallic crystal structure has its own coordination number, Z, which is the number of nearest neighbors surrounding a central atom. The crystal lattice is assumed to be composed entirely of "hard spheres" of identical radius so that all of the nearest neighbors "touch" the central atom they surround. The unit cell geometries for the bcc and fcc metals are shown in Figures 1A and 2A. The coordination numbers for these two crystal structures are

$$Z(\mathrm{bcc}) = 8 \qquad Z(\mathrm{fcc}) = 12 \tag{2}$$

Because the removal of one atom from a metallic lattice causes the breaking of Z bonds, it is tempting, but *not* correct, to assume that $\Delta_a U = Z\varepsilon$, where ε is the molar bond energy. It is true that the Z bonds surrounding this atom are broken during atomization; however, this process also breaks one of the Z bonds on each of the adjoining nearest-neighbor atoms. Thus, the ratio of bonds to atoms in a metallic lattice must be less than Z. The correct ratio is $Z/2$, because although each atom is bonded to Z nearest neighbors, each bond has an atom on each of the two ends. Hence, the actual ratio, after correcting for double counting, is $Z/2$.

Another way to obtain this result is to picture the gaseous M atoms in eq 1 as having Z half-bonds or "broken bonds" still attached to each atom. Of course, Z half-bonds is the same as $Z/2$ full bonds, again leading to the result that in a large crystal lattice of a pure metal there are $Z/2$ bonds for every one atom. Thus, for a metallic lattice, the molar bond energy, ε, can be found from the equation

$$\Delta_a U = \frac{Z}{2}\varepsilon \tag{3}$$

Equation 3 is based on the assumption that all of the bonding in the lattice is between nearest-neighbor atoms and that no interactions exist between more distant neighbors. This assumption is identical to that usually employed when bond energies are calculated for molecular substances.

Because the molar enthalpy is defined as $H = U + pV$, where V is the molar volume, and because the metallic vapor is an ideal gas, the standard molar lattice energy can be obtained from

$$\Delta_a H = \Delta_a U + RT \tag{4}$$

To illustrate the use of eqs 2−4 with bcc metals, chromium is selected with $Z = 8$ and a molar enthalpy of atomization of $\Delta_a H = 396.6$ kJ mol^{-1} at 25 °C *(3)*. The molar lattice energy is then $\Delta_a U = \Delta_a H - RT = 394.12$ kJ mol^{-1}. Thus, the energy of the chromium-chromium metallic bond is

$$\varepsilon(\mathrm{Cr}) = (394.12\ \mathrm{kJ\ mol^{-1}})/4 = 98.53\ \mathrm{kJ\ mol^{-1}}$$

10.1021/ed100189v Published on Web 04/12/2010

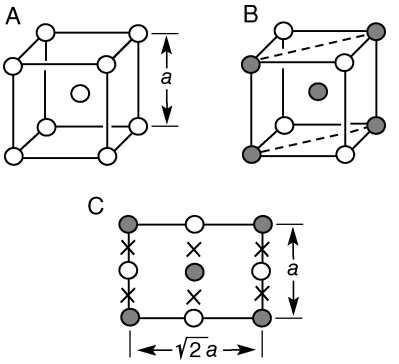

Figure 1. (A) The bcc unit cell with a coordination number of 8. (B) The (110) plane in the bcc cell (atoms in the plane are indicated with shaded circles). (C) Perpendicular view of the same (110) plane (atoms indicated with shaded circles), an adjacent (110) plane (atoms indicated with open circles), and the intersection of a third plane midway between these two planes with the bonds between the atoms in the two planes (intersections indicated with an ×).

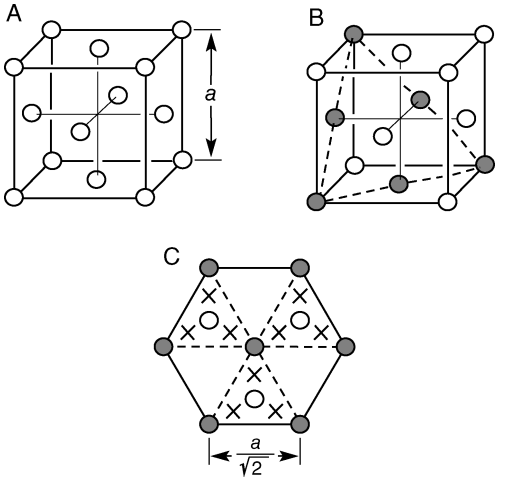

Figure 2. (A) The fcc unit cell. The coordination number is 12. (B) The (111) plane in the fcc cell (atoms in the plane are indicated with shaded circles). (C) Perpendicular view of the same (111) plane (atoms indicated with shaded circles), an adjacent (111) plane (atoms indicated with open circles), and the intersection of a third plane midway between these two planes with the bonds between the atoms in the two planes (intersections indicated with an ×).

The same approach is employed with fcc metals, as illustrated with copper. Here $Z = 12$, $\Delta_a H = 338.32$ kJ mol^{-1} *(3)*, $\Delta_a U = 335.84$ kJ mol^{-1}, and the copper-copper metallic bond has an energy of

$$\varepsilon(\mathrm{Cu}) = (335.84\ \mathrm{kJ\ mol^{-1}})/6 = 55.97\ \mathrm{kJ\ mol^{-1}}$$

We note that in discussions of covalent bonds, some texts actually provide bond enthalpies rather than bond energies *(2)*. Both are convenient for the estimation of the energy or enthalpy change in a chemical reaction, and as in the case of metallic bonds, there is not a great deal of numerical difference between the two.

The lattice energies and the bond energies for a variety of bcc and fcc metals, all calculated in the above fashion, are shown in Tables 1 and 2. Also included is the lattice constant, *a*, for each metal *(3)* and the bond length, *R*, for nearest-neighbor bonds that is obtained from the unit cell geometries in Figures 1A and 2A,

$$R(\mathrm{bcc}) = \frac{\sqrt{3}}{2}a \qquad (5)$$

$$R(\mathrm{fcc}) = \frac{a}{\sqrt{2}}$$

Table 1. Bond Energies and Bond Lengths for Various Bcc Metals

Metal	$\Delta_a H$/(kJ mol^{-1})	$\Delta_a U$/(kJ mol^{-1})	ε/(kJ mol^{-1})	*a*/pm	*R*/pm
Li	159.37	156.89	39.22	351	303.98
K	89.24	86.76	21.69	533.4	461.94
V	514.21	511.73	127.93	302.4	261.89
Cr	396.6	394.12	98.53	288.46	249.81
Mn	280.7	278.22	69.56	891.39	771.97
Fe	416.3	413.82	103.46	286.645	248.24
Rb	80.88	78.40	19.60	562	486.71
Nb	725.9	723.42	180.86	329.86	285.67
Mo	658.1	655.62	163.91	314.7	272.54
Cs	76.065	73.59	18.40	614	531.74
Ba	180	177.52	44.38	502.5	435.18
Ta	782	779.52	194.88	330.29	286.04
W	849.4	846.92	211.73	316.522	274.12

Table 2. Bond Energies and Bond Lengths for Various Fcc Metals

Metal	$\Delta_a H$/(kJ mol^{-1})	$\Delta_a U$/(kJ mol^{-1})	ε/(kJ mol^{-1})	*a*/pm	*R*/pm
Al	326.4	323.9	53.99	404.959	286.35
Ca	178.2	175.7	29.29	558.84	395.16
Co	424.7	422.2	70.37	354.41	250.61
Ni	429.7	427.2	71.20	352.38	249.17
Cu	338.32	335.8	55.97	361.47	255.60
Sr	164.4	161.9	26.99	608.49	430.27
Rh	556.9	554.4	92.40	380.36	268.96
Pd	378.2	375.7	62.62	389.08	275.12
Ag	284.55	282.1	47.01	408.626	288.94
Ir	665.3	662.8	110.47	383.92	271.47
Pt	565.30	562.8	93.80	392.40	277.47
Au	336.1	333.6	55.60	407.833	288.38
Pb	195	192.5	32.09	495	350.02

We note here that the metallic bond energies are generally somewhat smaller than the covalent bond energies found in most molecular or polymeric substances *(2)*. Students sometimes find it difficult to reconcile the high tensile strength of metals with the fact that metallic bond energies are somewhat lower than covalent bond energies. A simple explanation is that the metal lattice has a much larger number of bonds per atom than do most covalently bonded solids.

Bond Energies for the Hcp Metals

The calculation of the bond energy for the hcp metal crystal structure is not as straightforward as for the bcc and fcc metals.

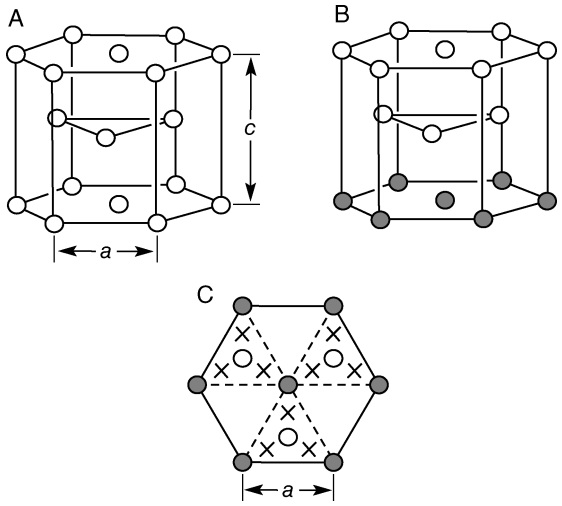

Figure 3. (A) The hcp unit cell. The coordination number is 12. (B) The (0001) plane in the hcp cell (atoms indicated with shaded circles). (C) Perpendicular view of the same (0001) plane (atoms indicated with shaded circles), an adjacent (0001) plane (atoms indicated with open circles), and the intersection of a third plane midway between these two planes with the bonds between the atoms in the two planes (intersections indicated with an ×).

The *theoretical* hcp unit cell with its coordination number of 12, which is identical to the coordination number of fcc metals, and two lattice constants a and c are shown in Figure 3A. In the fcc structure, all of the atoms are surrounded by 12 nearest neighbors that touch the central atom and all of the 12 resulting bonds are thus identical. The problem for the hcp metals is that none of them display the theoretical ratio of the two lattice constants, namely, $c/a = 2(2/3)^{1/2} = 1.633$ *(4)*, based on the geometry. In actuality, some hcp metals have a higher-than-theoretical ratio, whereas others display a lower-than-theoretical ratio *(4)*.

These two possibilities are most easily visualized if the central atom is pictured as the atom in the center of the basal plane of the unit cell shown shaded in Figure 3B. Thus, for hcp metals where c/a is larger than the theoretical value, it is only within the planes parallel to the basal plane that the atoms actually touch, whereas there is no touching between atoms occupying parallel, adjacent basal planes. Conversely, for hcp metals where c/a is less than the theoretical value, there is no atomic contact within the planes parallel to the basal plane, but there is contact between atoms occupying parallel, adjacent basal planes. Thus, in hcp metals, only 6 of the 12 surrounding atoms are *true* nearest neighbors (that touch the central atom), whereas the other 6 are slightly more distant atoms (and do not touch the central atom). As a result, there are two somewhat different "nearest-neighbor bonds" with differing bond energies and bond lengths, rather than only one. The lengths of these two bonds can be seen from the geometry of Figure 3A to be

$$R_b(\text{hcp}) = a \qquad (6)$$

$$R_n(\text{hcp}) = \sqrt{\frac{a^2}{3} + \frac{c^2}{4}}$$

where R_b represents the length of the bonds that are parallel to the basal plane and R_n is the length of the bonds that are not.

Presumably, a calculation based on eq 3 with $Z = 12$ would yield an average, ε_{av}, of the energy of the bonds parallel to the basal plane, ε_b, and those that are not, ε_n. This approximation, based on the theoretical value of the c/a ratio, will be employed here for the purpose of subsequent bond-energy and surface-energy calculations. The approximation seems to be justified by the reasonably good agreement between experimental and predicted surface energies for the hcp metals considered here. Hcp titanium is used to illustrate the calculation of ε_{av} for a hcp metal. Using $\Delta_a H = 469.9$ kJ mol^{-1} *(3)* and the approximation $Z = 12$, $\Delta_a U = 467.42$ kJ mol^{-1} and

$$\varepsilon_{av}(\text{Ti}) = (467.42 \text{ kJ mol}^{-1})/6 = 77.90 \text{ kJ mol}^{-1}$$

The average bond energy for a variety of hcp metals as well as the lattice constants *(3)* and their ratio c/a are shown in Table 3. Neither of the two bond lengths are calculated from eq 6 because neither length corresponds to the "average bond".

Surface Tension and Surface Energy

The surface tension, γ, of a solid can be simply defined as the work required to create new surface area (at constant temperature, volume, and composition) divided by the area created in the process. The surface tension, γ, is related to the surface free energy, f, through the equation $\gamma = f + \Sigma_i \mu_i \Gamma_i$, where μ_i and Γ_i are the chemical potential and the surface excess concentration of the ith component, respectively *(5, 6)*. For a pure substance and a planar interface, the Gibbs dividing surface can be located so that $\Gamma = 0$ and then

$$\gamma = f = u - Ts = \gamma_0 + T\frac{d\gamma}{dT} \qquad (7)$$

where $u = \gamma_0$ is the surface energy or the surface tension at absolute zero and $s = -d\gamma/dT$ is the surface entropy. If γ decreases linearly with temperature, as it commonly does, then γ_0 and $d\gamma/dT$ are both constant. Regardless of whether the temperature dependence of γ is linear or nonlinear, γ_0 can be found by extrapolation of the surface-tension data *(7, 8)* to absolute zero. The extrapolation can be performed either directly from experimental data or through the observation that the temperature coefficient of the surface tension, $d\gamma/dT$, is usually constant and falls within the range of $d\gamma/dT = -(0.27 \pm 0.07) \times 10^{-3}$ J m^{-2} K^{-1} *(7, 9)* for most metals. An alternative approach exists for finding γ_0 and γ for a solid metal by using liquid metal data and rather simple theoretical arguments for the estimation of γ and γ_0 for the solid metal *(10)*. Clearly, for metals at room temperature, the difference between γ and γ_0 is often small and is, in fact, sometimes ignored.

Surface-Energy Estimations for Bcc, Fcc, and Hcp Metals

The surface energy of a solid metal can be easily estimated from the bond energy, ε, and the experimental lattice constants for the metal. This approach is often referred to as the *broken-bond model* of surface energy and has been successfully employed for many years in estimating surface tensions and in understanding the much-noticed correlation between the surface tension or surface energy and the sublimation energy of metals *(9, 11, 12)*. The process can be visualized as the cleavage of the solid along a particular crystallographic plane. According to the broken-bond model, this work can be estimated by counting up the total energy of the bonds broken

Table 3. Bond Energies and Lattice Constant Ratios for Various Hcp Metals

Metal	$\Delta_a H$/(kJ mol^{-1})	$\Delta_a U$/(kJ mol^{-1})	ε_{av}/(kJ mol^{-1})	a/pm	c/pm	c/a
Be	324.6	322.1	53.69	228.55	358.32	1.5678
Mg	147.7	145.2	24.20	320.94	521.03	1.6234
Sc	377.8	375.3	62.55	330.9	527.3	1.5935
Ti	469.9	467.4	77.90	295.11	468.43	1.5873
Zn	130.729	128.3	21.38	266.47	494.69	1.8565
Y	421.3	418.8	69.80	364.74	573.06	1.5711
Zr	608.8	606.3	101.05	323.21	514.77	1.5927
Tc	678	675.5	112.59	274.3	440	1.6041
Ru	642.7	640.2	106.70	270.58	428.11	1.5822
Cd	112.01	109.5	18.26	297.94	561.86	1.8858
Hf	619.2	616.7	102.79	319.46	505.1	1.5811
Re	769.9	767.4	127.90	276.09	445.76	1.6145
Os	791	788.5	131.42	273.43	432	1.5799

in the process. The appropriate area can be found from the lattice constant for the metal.

The surface tension depends on the particular crystallographic plane along which the cleavage is envisioned. The plane selected for this calculation is the most stable plane, which is the plane with the lowest surface tension (because of free energy minimization). These planes are singular or atomically smooth planes that are also the closest-packed plane and are usually the slip plane *(13)*.

For the bcc structure, the closest-packed plane is the (110) plane. This plane (with its shaded atoms) is shown is Figure 1B, whereas the arrangement of atoms in the same plane and an adjacent parallel plane is shown in Figure 1C. The location of the intersection of the bonds between the two, adjacent layers with a plane midway between the two layers is marked with an ×. These intersections are thought of as the points of bond breakage. This atomic plane can be replicated via the rectangular surface unit cell shown in Figure 1C, which has an area of $2^{1/2}a^2$. The number of broken bonds within the rectangle is $2 + 4(1/2) = 4$. Thus, because two of these areas are formed during cleavage,

$$2\sqrt{2}a^2\gamma_0(\text{bcc}) = \frac{4\varepsilon}{L} \qquad (8)$$

$$\gamma_0(\text{bcc}) = \frac{\sqrt{2}\varepsilon}{La^2}$$

where $L = 6.02214 \times 10^{23}$ mol^{-1} is the Avogadro constant. The estimation of a surface energy from eq 8 is illustrated for bcc Cr, using the previous value of $\varepsilon = 98.53$ kJ mol^{-1} $= 98.53 \times 10^3$ J mol^{-1} and the experimental lattice constant of $a = 288.46$ pm $= 288.46 \times 10^{-12}$ m, yielding

$$\gamma_0(\text{Cr}) = 2.780 \text{ J m}^{-2}$$

This estimate is in excellent agreement with the experimental surface tension of $\gamma(\text{Cr}) = 2.400$ J m^{-2} *(14)* at 1600 °C and a surface energy from eq 7 of

$$\gamma_0(\text{Cr}) = [2.400 + (1873)(0.27 \times 10^{-3})] \text{ J m}^{-2}$$

$$= 2.91 \text{ J m}^{-2}$$

For the fcc structure, the closest-packed plane is the (111) plane, which is shown in Figures 2B and 2C. Again Figure 2C shows two adjacent atomic layers, along with the intersection of a plane midway between the layers with the bonds between the layers. This atomic plane can be replicated via the hexagonal surface unit cell shown in Figure 1C. (Technically, the surface unit cell is actually a parallelogram made up of two adjacent equilateral triangles out of the six shown in the hexagon.) The area of a regular hexagon with an edge length of l is $(3\cdot 3^{1/2}/2)l^2$. Because $l = a/2^{1/2}$, the area expressed in terms of the lattice constant is $(3\cdot 3^{1/2}/4)a^2$. The hexagon contains 9 broken bonds, so that the surface energy can be found from

$$2\left(3\frac{\sqrt{3}}{4}\right)a^2\gamma_0(\text{fcc}) = \frac{9\varepsilon}{L} \qquad (9)$$

$$\gamma_0(\text{fcc}) = \frac{2\sqrt{3}\varepsilon}{La^2}$$

The use of eq 9 is illustrated with fcc Cu, using the previous value of $\varepsilon = 55.97$ kJ mol^{-1} and the experimental lattice constant of $a = 361.47$ pm, yielding

$$\gamma_0(\text{Cu}) = 2.46 \text{ J m}^{-2}$$

which is in fairly good agreement with the experiment value of 1.78 J m^{-2} *(10)*.

For the hcp structure, the closest-packed plane is the (0001) or basal plane, which is shown in Figures 3B and 3C. The two adjacent atomic layers are shown in Figure 3C, along with the intersection of a plane midway between the layers with the bonds between the layers. The surface unit cell is similar to that in Figure 2C except that in this case the length of the edge of the regular hexagon is $l = a$, so that the area of the hexagon is $(3\cdot 3^{1/2}/2)a^2$. Thus, the surface energy can be found from

$$2\left(3\frac{\sqrt{3}}{2}\right)a^2\gamma_0(\text{hcp}) = \frac{9\varepsilon_{av}}{L} \qquad (10)$$

$$\gamma_0(\text{hcp}) = \frac{\sqrt{3}\varepsilon_{av}}{La^2}$$

The use of eq 10 is illustrated with hcp Ti, using the previous value of $\varepsilon_{av} = 77.904$ kJ mol^{-1} and the experimental lattice

constant of a = 295.11 pm, yielding

$$\gamma_0(\mathrm{Ti}) = 2.573\ \mathrm{J\ m^{-2}}$$

which is in fairly good agreement with the experimental value of 2.08 J m^{-2} *(10)*.

In the above surface-energy calculations, the error of the various estimates ranges from 4 to 40%. The error estimates should not be taken too literally, however, because of (i) the lengthy extrapolation required of the experimental data to absolute zero and (ii) the notoriously problematic nature of liquid or solid metal surface-tension measurements because of the difficulty in obtaining metallic surfaces that are not contaminated by impurities *(9)*. In addition, some of the assumptions of the model oversimplify metallic binding, in particular that (i) only nearest-neighbor interactions are important and (ii) surface bonds have the same strength as those in the interior of the solid, despite differences in coordination number. Note that if either eq 8, 9, or 10 is combined with eq 3, it is apparent that $a^2\gamma_0$ is proportional to $\Delta_a U$. This correlation was observed many years ago *(9, 11, 12)* and is a major part of the justification for viewing metallic bonding in a way that is similar to covalent bonding. Of course, there are other phenomena that further justify this metallic bonding approach to the interpretation of surface and bulk properties *(15)*.

Conclusion

It has been shown that the lattice energy, crystal structure, and coordination number of a metal can be used to calculate the bond energy of metallic solids. Once obtained, these bond energies can then be employed to make reasonable estimates of the surface energy of the closest-packed (and most stable) crystallographic plane of the solid. This procedure illustrates, on a fairly elementary level, the possibility of predicting material properties from knowledge of the interatomic or intermolecular interaction energy, which is one of the primary goals of materials science.

Literature Cited

1. See, for example , Somorjai, G. A. *Introduction to Surface Chemistry and Catalysis*; John Wiley & Sons: New York, 1994.
2. See, for example , Levine, I. A. *Physical Chemistry*, 5th ed.; McGraw-Hill: New York, 2002; pp 166−167 and 680−681.
3. Emsley, J. *The Elements*, 3rd ed.; Oxford University Press: Oxford, 1998.
4. Smith, W. F. *Foundations of Materials Science and Engineering*, 3rd ed.; McGraw-Hill: New York, 2004; pp 73−77.
5. Johnson, R. E., Jr. *J. Phys. Chem.* **1959**, *63*, 1655–1658.
6. Hudson, J. B. *Surface Science: An Introduction*; John Wiley & Sons: New York, 1992; pp 89−93.
7. Murr, L. E. *Interfacial Phenomena in Metals and Alloys*; Addison-Wesley Publishing Co.: Reading, PA, 1975; pp 122−125.
8. *Handbook of Physical Quantities*; Grigoriev, I. S., Meilikhov, E. Z., Eds.; CRC Press: Boca Raton, FL, 1997; p 417.
9. Allen, B. C. *Trans. AIME* **1963**, *227*, 1175–1183.
10. Tyson, W. R.; Miller, W. A. *Surf. Sci.* **1977**, *62*, 267–276.
11. Somorjai, G. A. *Introduction to Surface Chemistry and Catalysis*; John Wiley & Sons: New York, 1994; p 273.
12. Skapski, A. S. *J. Chem. Phys.* **1948**, *16*, 389–393.
13. Smith, W. F. *Foundations of Materials Science and Engineering*, 3rd ed.; McGraw-Hill: New York, 2004; pp 211−216.
14. Allen, B. C. *Trans. AIME* **1969**, *245*, 1621–1632.
15. See, for example , Somorjai, G. A. *Introduction to Surface Chemistry and Catalysis*; John Wiley & Sons: New York, 1994; pp 400−441.

